AD________________

Award Number: DAMD17-00-1-0716

TITLE: Foot and Ankle Injuries in the Military

PRINCIPAL INVESTIGATOR: Mark D. Grabiner, Ph.D.

CONTRACTING ORGANIZATION: The Cleveland Clinic Foundation
Cleveland, Ohio 44195

REPORT DATE: October 2002

TYPE OF REPORT: Annual

PREPARED FOR: U.S. Army Medical Research and Materiel Command
Fort Detrick, Maryland 21702-5012

REPORT DOCUMENTATION PAGE

Form Approved
OMB No. 074-0188

1. AGENCY USE ONLY (Leave blank)	2. REPORT DATE	3. REPORT TYPE AND DATES COVERED
	October 2002	Annual (1 Oct 00 - 30 Sep 02)

4. TITLE AND SUBTITLE
Foot and Ankle Injuries in the Military

5. FUNDING NUMBERS
DAMD17-00-1-0716

6. AUTHOR(S)
Mark D. Grabiner, Ph.D.

7. PERFORMING ORGANIZATION NAME(S) AND ADDRESS(ES)
The Cleveland Clinic Foundation
Cleveland, Ohio 44195

E-Mail: grabiner@bme.ri.ccf.org

8. PERFORMING ORGANIZATION REPORT NUMBER

9. SPONSORING / MONITORING AGENCY NAME(S) AND ADDRESS(ES)
U.S. Army Medical Research and Materiel Command
Fort Detrick, Maryland 21702-5012

10. SPONSORING / MONITORING AGENCY REPORT NUMBER

11. SUPPLEMENTARY NOTES

12a. DISTRIBUTION / AVAILABILITY STATEMENT
Approved for Public Release; Distribution Unlimited

12b. DISTRIBUTION CODE

13. ABSTRACT (Maximum 200 Words)

No Abstract Provided.

14. SUBJECT TERMS
Foot and Ankle Injuries

15. NUMBER OF PAGES
17

16. PRICE CODE

17. SECURITY CLASSIFICATION OF REPORT	18. SECURITY CLASSIFICATION OF THIS PAGE	19. SECURITY CLASSIFICATION OF ABSTRACT	20. LIMITATION OF ABSTRACT
Unclassified	Unclassified	Unclassified	Unlimited

Table of Contents

FOOT AND ANKLE INJURIES IN THE MILITARY
Program Director: M.D. Grabiner, PhD

Treadmill Study: Investigating the metatarsals/Longitudinal Arch

Methods:

25 males and 25 females between the ages of 18-27 without lower extremity injuries, flat feet, or arch deformities were recruited. All subjects were required to meet the standard physical prerequisites set forth by the local ROTC programs. Subjects walked on a dual track treadmill instrumented with force plates under two conditions: 1) Load: which required the subjects to wear a 20kg military type backpack with a metal frame and hip strap 2) Control: without any additional load. The order of these conditions was selected randomly and completed on two different dates. The subjects completed each of the conditions while in good health and wearing athletic shoes. Each condition began with a 5-minute warm-up at 4.8km/hr without the 20kg backpack. After the warm-up was complete the subject stepped down from the treadmill and removed his/her shoes. Footprints of both feet were made in order to measure arch index. Foot compliance measurements were also taken at this time including foot length, foot width, and arch height (measured from the tuberosity of the navicular to the floor) under 50% body weight. For load condition the subject was then fitted for the backpack. In each condition, the subject then resumed walking at 4.8 km/hr for another 5-minute period at the end of which treadmill speed increased to 6.4 km/hr for 60 minutes. During this hour long time period, six force plate data trails were collected at 5,11, 26, 41, 54 and 60 minutes at a frequency of 100Hz for 60 seconds using Adisoft collection software. This data was processed using a Matlab program to calculate peak vertical force, loading rate, and stride time. At the end of the 60-minute phase, the treadmill speed was decreased to 4.8 km/hr and the subject was allowed a 5-minute "cool down" session after which a second set of footprints were made and arch index and foot compliance measurements were obtained.

Preliminary Results:
The data showed that peak vertical force means were significantly higher (P < .001) with the backpack (1156.2 ± 151.2N) than without (886.7 ± 167.9 N). The loading rate was also significantly higher (P < .001) for the load condition (9234.6 ± 3768.1 N/sec) than for the control condition (5687.8 ± 3301.3 N/sec). Stride time was not significantly changed between conditions. This data validate the hypothesis that added load causes higher forces to be exerted underneath the feet at greater rates. However, it does not support the idea that this additional load causes human volunteers to alter their step kinetics and kinematics in such a manner that the metatarsals are loaded more frequently. Potentially due to fatigue, the before and after arch index measurements for the control condition were significantly different in both feet, $P_{right}\approx 0.001$ and $P_{left}\approx 0.014$ (See Chart A). Conversely, for the load condition the before and after measurements were only significantly different for the left foot ($P \approx 0.016$) and not for the right foot ($P\approx 0.8355$) (See Chart B). The reason behind this difference in conditions is yet to be determined.

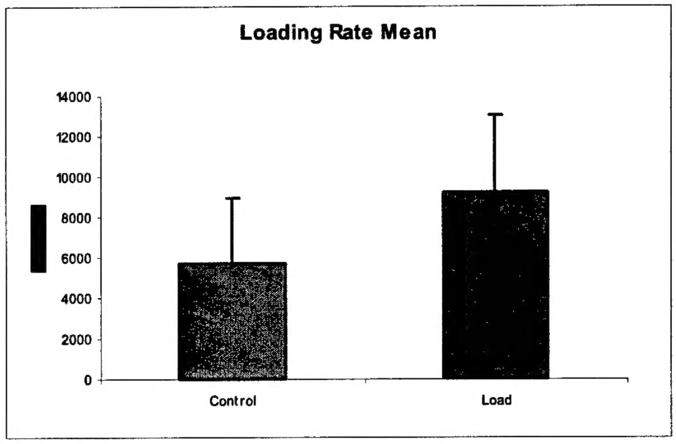

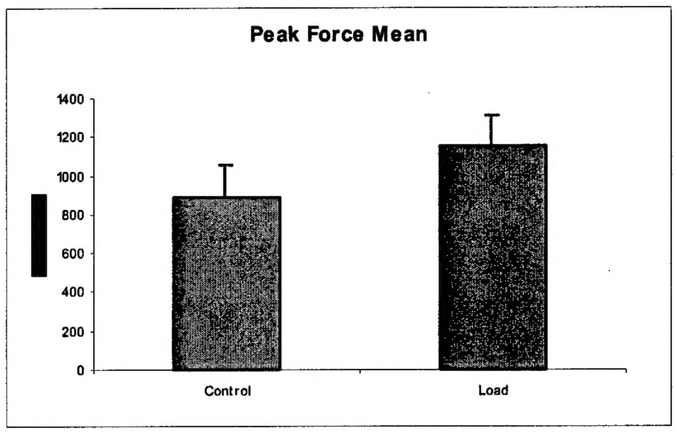

Control	Right		Left	
	Before	*After*	*Before*	*After*
Mean	0.684	0.657	0.719	0.697
Variance	0.033	0.038	0.052	0.061
	P=0.00147		P=0.0145	

Chart A

Load	Right		Left	
	Before	*After*	*Before*	*After*
Mean	0.684	0.682	0.717	0.689
Variance	0.037	0.037	0.060	0.069
	P=0.836		P=0.0162	

Chart B

Mechanisms underlying calcaneal fractures

Introduction

More than 80 % of military injuries occur in the lower extremities and the most frequent site of injury is the foot and ankle (Almeida *et al*, 1996). Calcaneal fractures are one of the serious and debilitating injuries, which are difficult to treat and rehabilitate. The severity of the injury is dependent on the type of fracture. The most difficult to manage are the intra-articular fractures which occur in seventy five percent of all calcaneal fracture cases.

Methods

Nondestructive biomechanical tests were performed on 14 unembalmed human cadaver legs (6 male, 8 female), aged 41 – 58 years, transected at the distal third of the tibia. The specimens were stored at – 20 °C and thawed 24 hrs before the testing was conducted. The proximal portion of each specimen's tibia was potted in a cylindrical tube using cerrobend alloy (also called as woods metal). The tests were conducted using a custom made jig designed to simulate the loading produced during landing from a parachute. The potted specimen was then attached to the jig with its plantar surface facing upwards.

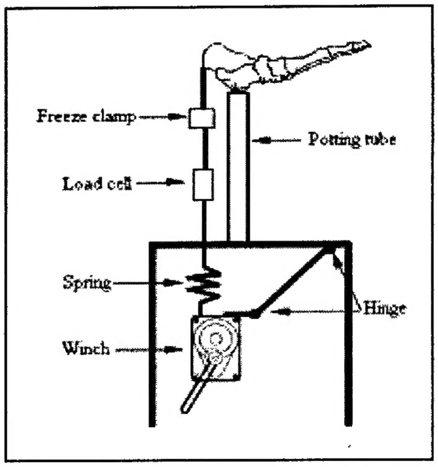

Figure 1 Achilles tendon - spring - winch arrangement

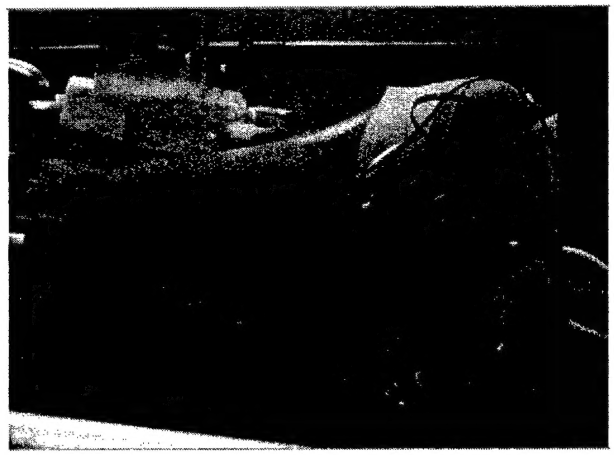

Figure 2 Bone extensometer

The jig was designed to apply dynamic axial loads to the plantar aspect of the foot using an impactor. The impact forces on the foot can be varied by altering the weight of the impactor or by adjusting the impactor release height. In order to position the foot prior to applying impact forces and to mimic the biomechanical conditions during impact, the Achilles tendon was connected to a mechanical compression spring of stiffness18.26 KN/m. The spring stiffness was selected according to the leg stiffness reported by Farley et al, 1999. A winch was used to tension the Achilles tendon according to different loading condition. The Achilles tendon – spring - winch arrangement along with instrumentation is shown in figure 1.

Bone strains in the lateral side of the calcaneus were measured using uniaxial strain gages and an extensometer. Global strain in the calcaneus was measured by six 10 mm gage length Capacitec® sensors attached to three intracortical pins (figure 2). Strains in the plantar aponeurosis were measured using omega transducers. To gain access to the calcaneal bone surface, a 5 cm x 4 cm incision was made on the lateral side of the calcaneus. The cortical bone surface was prepared for bonding the uniaxial strain gages by removing the periosteum using a scalpel and polishing the surface using sand paper. Uniaxial strain gages were bonded to the bone surface by using methyl-cyanoacrylate adhesive applied to the bone surface and by pressing down the uniaxial gage using cotton tipped applicator. Uniaxial load cells (A.L.Design, Buffalo, NY) were used to measure

the impact loads at the forefoot and hindfoot and were located just above the impacting surfaces (figure 3). Achilles tendon force was measured using a load cell (OMEGA Engineering, INC., Stamford, Connecticut) attached in series with the help of a freeze clamp. This custom made freeze clamp was cooled using solid carbon dioxide (otherwise called as dry ice) and is capable of withstanding tensile forces up to 3500 N (Figure 4).

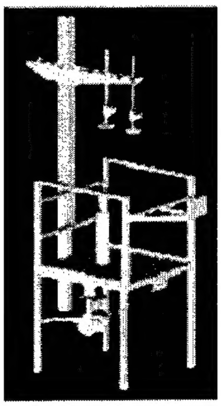

Figure 3

Figure 4

Loading condition:

The foot was tested using two different loading conditions.

(1) The Achilles tendon was loaded for two seconds with the fixed impactor constraining the fore foot. The experiment was repeated 10 times and the data were collected at 1000 Hz for 2 sec using a custom LabVIEW® program and filtered. The first 5 trials were collected with the extensometers on and the next five were collected with the extensometers on. This was done to minimize the noise in the uniaxial strain gage data.

(2) The forefoot was initially restrained and one second after tensioning the Achilles tendon an 8 kg impactor was released using a magnetic release mechanism, from a height of 15 cm. This made contact with the forefoot and 25 ms later with the hindfoot. Only the uniaxial strain gages were used to collect the bone strain data. The experiment was repeated 5 times and the data were collected at 2000 Hz for 4 sec using a custom LabVIEW® program and filtered.

Preliminary results

Typical maximum Achilles tendon forces experienced during the first loading condition were approximately 700 – 1000 N. The lateral strain inferior to the apex of Gissane's angle (measured using an uniaxial strain gage) experienced compression during the tensioning phase. As expected, the plantar aponeurosis experienced tension during the first loading condition. Further data analysis is required to find the effect of Achilles tendon force and heel impact force on calcaneal bending. Typical Achilles tendon force and strains were shown below.

Reference: Almeida SA, Williams KM, Shaffer RA, Brodine SK. An epidemiological study of the association between patterns of physical training and musculoskeletal injuries. Naval Health research publication 96 – 132, 1996.

Farley CT, Morgenroth DC. Leg stiffness primarily depends on ankle stiffness during human hopping. J Biomech. 1999 Mar; 32(3):267-273.

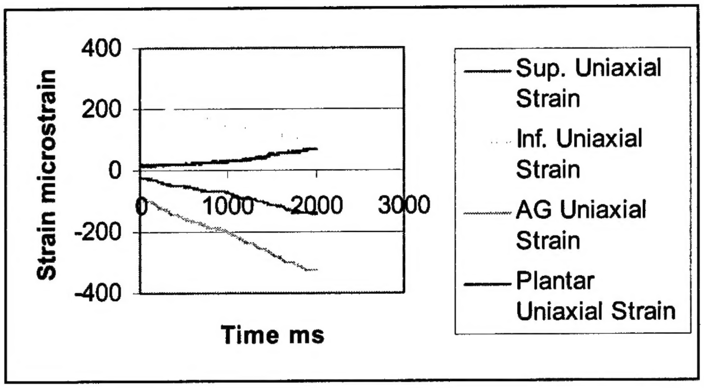
400
200
0
-200
-400
0
1000
2000
3000
Strain microstrain
Time ms
Sup. Uniaxial Strain
Inf. Uniaxial Strain
AG Uniaxial Strain
Plantar Uniaxial Strain

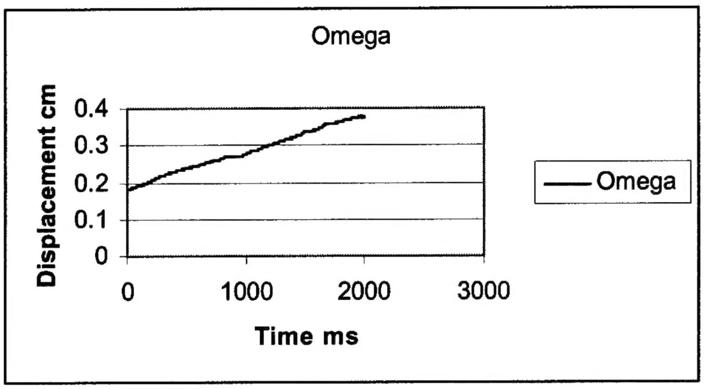
Omega
0.4
0.3
0.2
0.1
0
0
1000
2000
3000
Displacement cm
Time ms
Omega

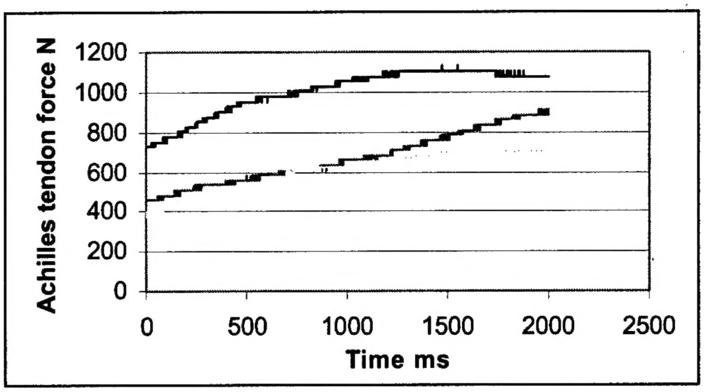
1200
1000
800
600
400
200
0
0
500
1000
1500
2000
2500
Achilles tendon force N
Time ms

Metatarsal Stress Fractures in the Military

Four Point Bending Study: Investigating metatarsal fatigue

February 24, 2002

(Study Period: In Progress)

Methods:

Second and third metatarsals were dissected from 25 unpaired fresh frozen cadaver feet. There were 11 male donors and 14 female donors of a mean age of 61 years (range 24-93 years). Specimens were wrapped in paper towels soaked in saline solution. They were kept frozen at -20° Celsius in airtight plastic bags until testing. Specimens were mechanically tested in four-point bending configuration using a servo hydraulic materials test system (MTS Bionix, Minneapolis, MN). The distance between the upper pair of loading point was constant between specimens at 12 mm and the lower pair of loading points was positioned at the epiphyses of the metatarsal bone. This distance was measured with calipers. Specimens were preloaded to 10 newtons (N) and then loaded cyclically for 20 cycles at 1.2 mm displacement. At the end of 20 cycles preload was reset to 10 newtons and the process was repeated until fracture.

Results:

Results are pending repair of MTS Bionix mechanical testing system (MTS Systems Corporation, Minneapolis, MN).

Figure 1: Metatarsal testing fixture.

Figure 2: Metatarsal breaking after fatigue

Foot and Ankle Injuries in the Military: Biomechanical Modeling

Computer modeling complements the human subject testing and in vitro testing components of this project. Human testing provides information about the performance of non-injurious movements by normal subjects and patients. In vitro testing allows simulation of injury, but does not include the aspects of active neuromuscular control and whole body inertia. The aims of the computer modeling work are: (1) to develop a three dimensional musculoskeletal model and validated simulations of vertical landing movements, (2) to use this model to determine the effect of neuromuscular control on the risk of ankle sprains when landing on an uneven surface, and (3) to use this model to determine the effect of neuromuscular control on the risk of heel fracture when landing from large heights.

Modeling pipeline

The experimental procotol was completed at the time of the previous progress report. Briefly, the subject jumps down from a height of 61 cm and runs forward. 3-D movement data is collected using a 6-camera video system at 240 fps (Motion Analysis Corp., Santa Rosa CA), and ground reaction forces from both feet using two force platforms (AMTI, Arlington VA). Data is also collected during standing, and the footprint is traced on paper.

The computational model has been completed. The model is implemented as a pipeline process, orchestrated by a Matlab script that performs the following functions without user intervention:

1. From the 3-D coordinates of body mounted markers during standing, a subject-specific scaled skeletal model is constructed. The model has 18 kinematic degrees of freedom and two legs.
2. The skeletal model is input into the Mocap Solver software (Motion Analysis Corp., Santa Rosa, CA) which solves the time histories of the bone motion from the marker trajectories recorded from the drop landing trials.
3. Mocap Solver exports the skeletal model, with inertial properties, as a .SD file which is used by SD/FAST (PTC, Needham MA) to generate dynamic equations of motion in C code. This C code is saved in a file SUBxxx.C, where xxx is the subject ID number.
4. Matlab takes muscle path models generated by SIMM (Musculographics, Evanston IL), scales them to the subject, and inserts these into the model using multivariate polynomial equations (Dhillon and van den Bogert, 2002).
5. Matlab scales mechanical properties of muscle (length of muscle fibers and tendon) to the subject.
6. Matlab converts the scanned footprint outline into a grid of 91 contact points under the foot, which will be used to generate ground contact forces.
7. Results of steps 4, 5, and 6 are saved on a text file SUBxxx.BIO.
8. Matlab takes the motion and ground reaction force data from 10 movement trials, synchronizes them, and computes an ensemble average and ensemble standard deviation for the first 200 ms after first ground contacts for the duration, resampled at 1 ms intervals.

9. Initial conditions (kinematic degrees of freedom, and their derivatives) are computed for t=0.

10. Results of steps 8 and 9 are saved on a text file SUBxxx.DAT

<u>Simulation software</u>

C code was written to perform movement optimizations and injury simulations. This code makes use of the in-house library SDBIO.C which provides a programming environment for biomechanical modeling and simulation using SD/FAST. The C code can function in one of five modes:

1. *Optimization.* The files SUBxxx.BIO and SUBxxx.DAT are read and muscle stimulation patterns are optimized using simulated annealing until the simulated movement agrees best with the subject's average motion and ground reaction forces. This typically requires 100,000 iterations of the movement simulation, and these are performed on the Linux/Mosix cluster. The optimized muscle stimulation patterns are written to a file SUBxxx.par for later use. Details of the simulated movements (kinematics, plantar pressure distributions, muscle forces, etc.) are also written to files for plotting.

2. *Validation.* The file SUBxxx.par is used to generate muscle stimulation patterns and ten simulations are performed, each one starting with the initial conditions of the skeleton (generalized coordinates and velocities) taken from an individual movement trial. The simulated movement is compared to the actual movement of the corresponding trial and errors are quantified. This tests the ability of the model to predict the consequences of changes in initial joint angles.

3. *Ankle sprain simulation.* 5000 simulations are performed, each one with an uneven ground surface. The ground surfaces are randomly generated by placing a "hole" with a Gaussian profile at a random location in a 20x30 cm rectangle, a random width of 5-20 cm, and a random depth of 0-10 cm. Ankle sprain was defined to occur at a supination moment of 34 N m (Parenteau, 1998). All results, input and output of each simulation, are logged and number of injuries recorded.

4. *Calcaneal fracture simulation.* The same 5000 simulations are performed, but with an 1.5 m/s increase in initial downward velocity. This corresponds to a real life situation where the surface is about 40 cm lower than expected, resulting in a larger impact velocity for which the subject is not prepared. Calcaneal fracture was defined as a case where the peak force on the rearfoot exceeds 8100 N (Levine et al., 1998). All results, input and output of each simulation, are logged and number of injuries recorded.

5. *Single simulation.* The muscle stimulation patterns are read from SUBxxx.par, and a single simulation is performed. This mode is used when it is necessary to repeat one of the 5000 injury simulations for more detailed study, generating full output with all model variables available for plotting, as in Mode 1.

<u>Postprocessing</u>

From each movement simulation, we can generate a movie of the plantar pressure distribution (Fig. 1), a 3-D interactive animation in VRML (Virtual Reality Modeling Language; Fig. 2), and graphs of all simulated variables, e.g. ground reaction forces (Fig. 3).

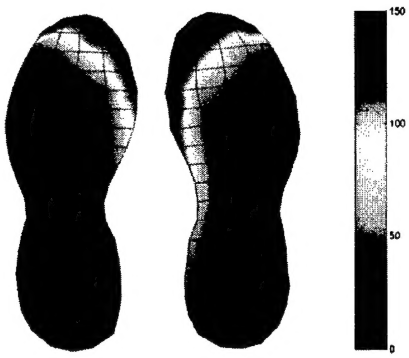

Figure 1: Snapshot from an animated display of simulated pressure distribution under the shoe. Pressure scals is in kPa.

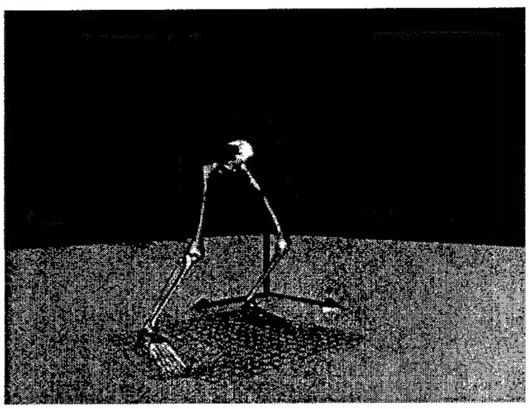

Figure 2: Example of a right ankle sprain on an uneven floor. Peak supination moment was 41 N m at *t* = 107 ms. Snapshot of a 3-D VRML animation.

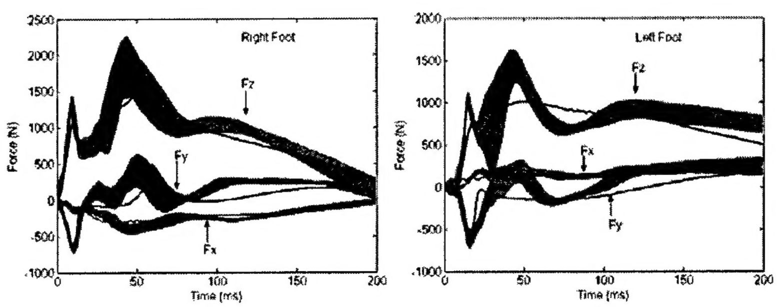

Figure 3: Simulated and measured ground reaction force. X is to the right, Y is to the front, and Z is vertical. Colored area represents mean ± SD of the 10 subject performances.

The VRML animations (Figure 2) can be viewed interactively in 3-D. Parallel Graphics Inc. (http://www.parallelgraphics.com) provides teh Cortona VRML viewer at no cost which can be installed as a plugin for Netscape, Microsoft Explorer, and Microsoft Powerpoint. The user can rotate, zoom, start and stop the movement. Variables of interest, e.g. the ligament load, can be animated together with the movement. This postprocessing system is an effective way to communicate and visualize the various injury mechanisms. This medium can facilitate injury prevention through education and awareness.

Validation results

Table 1: Model validation results. Two optimizations were performed (Model 1, Model 2). Each optimization resulted in almost identical movements and ground reaction forces, but with slightly different muscle activation strategies. RMSfit is the RMS (root

mean square) difference between the optimized simulation and the mean subject performance. It is normalized to the between-trial SD, so a value of 1 indicates that the model was within one standard deviation of the subject's performance, after optimization. RMSpred is the RMS difference between predicted and measured data, using initial conditions from each trial, without model re-optimization. All RMS errors were computed over 200 ms. Prediction of the injury-related variables (vertical force Fz and ankle supination Ay) is satisfactory.

	RMSfit/SD		RMSpred/SD	
	Model 1	Model 2	Model 1	Model 2
rightFx	1.17	1.12	2.13	2.14
rightFy	2.09	2.11	2.76	2.73
rightFz	1.20	1.16	2.66	2.67
leftFx	0.99	1.01	1.94	1.72
leftFy	1.91	1.89	2.12	2.39
leftFz	1.01	0.82	1.65	1.49
bodyRx	0.67	0.39	1.51	1.36
bodyRy	0.43	0.53	2.54	2.38
bodyRz	0.88	1.04	1.92	1.94
rightHx	0.56	0.52	2.18	2.10
rightHy	0.38	0.39	3.12	2.92
rightHz	0.59	0.64	1.90	2.07
rightKx	1.14	0.89	4.49	4.24
rightAx	1.30	1.37	3.08	3.73
rightAy	0.68	0.83	1.41	1.53
leftHx	0.38	0.40	1.91	1.83
leftHy	0.44	0.38	2.01	1.71
leftHz	0.73	0.74	2.56	2.51
leftKx	0.86	1.04	3.75	3.73
leftAx	1.44	1.62	3.51	3.33
leftAy	0.36	0.33	1.70	1.46

Injury experiments: Ankle sprain

The two optimized models gave similar results, both are presented in Table 2. When exposed to 5000 random uneven surfaces, the number of injuries ranged from 91 in the left ankle to 125 in the right ankle. The simulations were repeated with systematic changes in initial conditions to determine which changes in body posture would increase or decrease the risk of ankle sprain when landing on an unexpected uneven surface.

Table 2: Effect of changes in initial joint angles on the number of ankle sprains. Large increases in injury risk are highlighted in red, large decreases in green. Joint angles had a neglegible effect on injuries in the contralateral limb, so left ankle sprains are only reported for conditions in which joint angles in the left leg were altered, and right ankle sprains are reported for conditions in which joint angles in the right leg were altered.

Condition	Left ankle sprains		Right ankle sprains	
	Model 1	Model 2	Model 1	Model 2
Baseline	110	125	163	91
HipFlex –5°	[illegible]	[illegible]	[illegible]	[illegible]
HipFlex +5°	[illegible]	[illegible]	[illegible]	[illegible]
HipAbd –5°	108	131	143	97
HipAbd +5°	98	113	160	89
HipExtRot –5°	111	124	135	75
HipExtRot +5°	116	130	277	167
KneeExt –5°	[illegible]	[illegible]	[illegible]	[illegible]
KneeExt +5°	[illegible]	[illegible]	[illegible]	[illegible]
DorsiFlex –5°	104	119	[illegible]	[illegible]
DorsiFlex +5°	118	142	[illegible]	[illegible]
Eversion –5°	[illegible]	[illegible]	[illegible]	[illegible]
Eversion +5°	[illegible]	[illegible]	[illegible]	[illegible]
Vz +10%	127	128	[illegible]	[illegible]
Vz +20%	105	120	[illegible]	[illegible]
Vz +30%	90	106	[illegible]	[illegible]
Vz +40%	[illegible]	[illegible]	[illegible]	[illegible]
Vz +50%	[illegible]	[illegible]	[illegible]	[illegible]

Some clear patterns emerge from these results. As expected, the number of ankle sprains increases when the foot is more inverted during the landing. This is the case for both legs. All other results show a clear left-right difference, which must be seen in relation to the task that was performed. The task was a drop jump followed by running, which is typically performed asymmetrically. The right foot contacted the ground first (Figure 3), and the left foot was placed more forward. The number of injuries decreases dramatically if the left hip is more extended and the right hip is more flexed. The number of injuries also decreases when the left knee is more flexed and the right knee is more extended at impact. This implies that the risk of injury is smallest when foot placement is symmetrical, with feet side by side and not one in front of the other. When landing velocity (Vz) is increased more than 40%, there is a large risk of injury in left ankle. Surprisingly, injury risk in the right ankle is decreased at the same time.

For this injury scenario, with 5000 uneven surfaces, the effect of initial knee and hip flexion, i.e. forward-backward foot placement, is much larger than the effect of initial ankle angles. These hip and knee effects are also opposite in both limbs. Both of these results were surprising and important for injury prevention.

Injury experiments: Calcaneal fracture

When the landing velocity was increased by 1.5 m/s, 68% of the 5000 landings resulted in a right heel fracture, and 74% resulted in a left heel fracture. Obviously, many landings caused a bilateral calcaneal fracture. Sensitivity analyses, analogous to those for ankle sprains (Table 2) are in progress.

Plans for the remainder of the project

1. The results of Table 2 will be confirmed with models based on other human subjects.
2. The mechanisms responsible for the results in Table 2 will be further studied, by looking in detail at forces and kinematics to explain the asymmetry in results.
3. Sensitivity analyses will be performed for calcaneal fractures to identify influence of initial joint angles and muscle activation on the risk of calcaneal fracture.

Publications and presentations

Dhillon GS, van den Bogert AJ (accepted for publication) An efficient method for modeling of muscle moment arms. *Journal of Biomechanics.*

Huang X, McLean SG, Su A, van den Bogert AJ (2003) A musculoskeletal model for simulation of ankle sprains during two-legged landing movements. *Annual Meeting of the American Society for Biomechanics*, Toledo OH.

van den Bogert AJ, Su A, McLean SG, Huang X (2002) Forward dynamic modeling of acute injury: effective methods for optimization, validation, and experimentation. *IVth World Congress of Biomechanics*, Calgary, Canada.